Available online at www.sciencedirect.com
SCIENCE DIRECT®
Journal of Nuclear Materials 348 (2006) 165–173
journal of nuclear materials
www.elsevier.com/locate/jnucmat

Effect of residual carbon on the sintering behavior of MOX pellets

K. Asakura *, K. Takeuchi

Plutonium Fuel Center, Tokai-Works, Japan Nuclear Cycle Development Institute, Tokai-mura, Naka-gun, Ibaraki-ken 319-1194, Japan

Received 7 March 2005; accepted 23 September 2005

Abstract

Sintering behavior of MOX compacts containing different amounts of carbon (290–1735 ppm) was investigated at temperatures from 1073 to 2023 K to study the effect of residual carbon. Specimen shrinkages were measured with a non-contact type optical dilatometer during heating. The compact shrinkage at temperatures from 1273 to 1523 K was about six times larger in the two specimens with high residual carbon content than in the two with low content. This behavior could be understood by considering that shrinkage of the former specimens was enhanced in this temperature range by the decrease of O/M ratio due to the evolution of CO gas and consequently the significant increase of the metal ion inter-diffusion coefficient. In the specimens with low residual carbon content, the amount of CO gas evolution was too small to affect the inter-diffusion coefficient. This difference in shrinkage between the two kinds of specimens was also discussed from a theoretical model applied to the initial sintering stage of ceramics.

PACS: 89.02

1. Introduction

In the fast breeder reactor (FBR), it is critical to irradiate fuel to high burn-up beyond 100 GWd/t. Large swelling and fission gas release in the mixed oxide (MOX) fuel irradiated to high burn-up significantly affect the fuel performances such as the fuel-cladding mechanical interaction (FCMI) and the increase of internal pressure in fuel pins.

Several techniques to fabricate MOX fuel pellets have been developed [1–5]. Most have targeted fabrication of high density pellets with over 95% theoretical density. When high density pellets are used in the fuel pins, it is difficult to alleviate the FCMI caused by the fuel swelling and to reduce the internal pressure in the fuel pins during irradiation. MOX fuel pellets of low density are expected to effectively reduce these effects and improve the fuel performance. There are two approaches to fabricate these pellets: One is to sinter the pellets at low temperature, and the other is to form a number of stable pores in the pellet by using a powder containing an organic additive (hereafter referred to as pore former) [6]. The first approach is not so good, because the pellets are unstable and consequently densification takes place at low burn-up. Then, the

* Corresponding author. Tel.: +81 29 282 3320; fax: +81 29 282 3326.
E-mail address: asakura@tokai.jnc.go.jp (K. Asakura).

0022-3115/$ - see front matter © 2005 Elsevier B.V. All rights reserved.
doi:10.1016/j.jnucmat.2005.09.016

latter approach is preferably utilized in Japan for pellet fabrication.

A pore former is homogeneously mixed into MOX powder and then mixed powder is pressed into a green pellet. This pore former is decomposed and removed from the pellet matrix by the de-waxing heat treatment at about 1073 K, resulting in the homogeneous distribution of pores in the pellet matrix during the following sintering operation at about 1973 K. Paraffin or cellulose is generally utilized as the pore former because they have a relatively low decomposition temperature. Even after a well-worked de-waxing, however, certain amounts of carbon still remain in the de-waxed MOX green pellet. It is not known how this residual carbon affects the sintering behavior; on the other hand, it is known that the doping of small amounts of impurity elements such as niobium and rare earth metals can enhance the sintering and grain growth in UO_2 pellets [7,8]. It is therefore important to understand the effect of residual carbon on the sintering behavior of MOX pellets.

In this study, the sintering behavior of MOX pellets having four different amounts of residual carbon was investigated at temperatures from 1073 to 2023 K. The shrinkage rates of de-waxed MOX green pellets were measured by dilatometric analysis during the gradual temperature increase up to 2023 K. The observed differences in sintering behavior were discussed from the viewpoint of oxygen potential change during heating.

2. Experimental

2.1. Preparation and heat treatment of green pellets

Fig. 1 shows the flow sheet to obtain the de-waxed MOX green pellets containing different amounts of carbon. First, MOX powder, ADU (ammonium diuranate) UO_2 powder and recycled MOX powder were weighed and mixed in the ball mill developed by Japan Nuclear Cycle Development Institute (JNC). The mixing gave a homogeneous distribution of UO_2 and PuO_2 powders. The MOX powder was directly converted by microwave heating of the mixed solutions of uranyl nitrate and plutonium nitrate (hereafter MH–MOX powder). The internal surface of the ball mill was lined with silicon rubber and alumina balls were used as a mixing medium to easily control the powder characteristics [9].

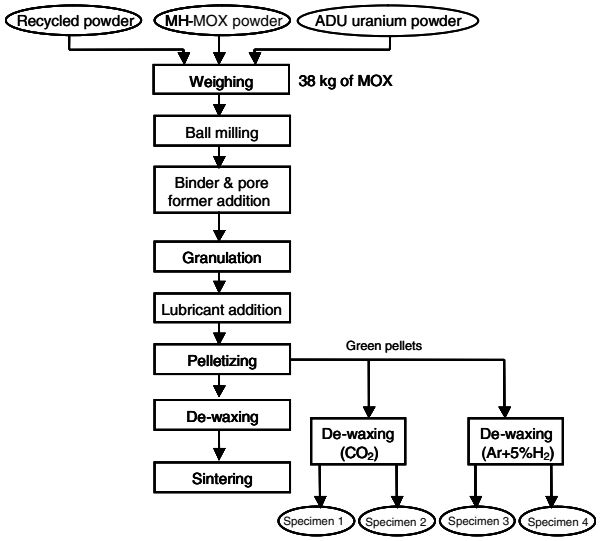

Fig. 1. Flow sheet of process for preparing the specimens.

After the ball milling, the binder and pore former were added into and blended with the powder obtained by a delta mixer. This powder was compacted by a roll press, crushed to give another powder, and then sieved to obtain good flowability. This powder was pressed into green pellets at a pressure of 5 t/cm^2 after mixing with a lubricant in the delta mixer. The amounts of binder, lubricant and pore former are shown in Table 1. The green pellets with 1.0 and 1.2 wt% contents of pore former were heated to 1073 K at a heating rate of 200 K/h, kept at this temperature for 2.5 h, and then cooled down to room temperature at the same heating rate to

Table 1
Dewaxing atmosphere and contents of plutonium, additives and residual carbon

Specimen no.	Plutonium content (wt%)	Zinc stearate content (wt%)		Pore former content (wt%)	Dewaxing atmosphere	Carbon content after dewaxing (ppm)
		Binder	Lubricant			
Specimen 1	24.8	0.5	0.2	1.0	CO_2	290
Specimen 2	25.5			1.2	CO_2	560
Specimen 3	24.8			1.0	Ar + 5% H_2	1730
Specimen 4	25.5			1.2	Ar + 5% H_2	1735

remove additives. Two different atmospheres were used in the de-waxing: carbon dioxide (CO_2) gas and argon gas containing 5% hydrogen (Ar + 5% H_2). As shown in Table 1, the difference in oxidation ability of the pore former in the two atmospheres resulted in significantly different contents of residual carbon. The carbon content was measured by infrared analysis.

2.2. Procedure

Four specimens (Table 1) were used to investigate the effect of residual carbon on the sintering behavior of the MOX pellets containing about 25 wt% of plutonium. They were classified into two groups: specimens 1 and 2 had low residual carbon content, and specimens 3 and 4 had high content.

Fig. 2 shows a schematic diagram of the apparatus used. The specimen shrinkage during heating was measured with a non-contact type optical dilatometer. The shadow of a heated specimen was projected into the scope by light irradiation from a halogen lamp, and then images of the top and bottom ends were enlarged using the scope lens. The change of distance between them showed the change of specimen length. The specimen shrinkage could be measured within an error of plus minus 20 μm at temperatures up to 2473 K.

The specimen was heated from room temperature to 2023 K at a heating rate of 400 K/h under an Ar + 5% H_2 atmosphere, which is the same as used in the mass production of MOX fuel pellets. From 1073 K, the specimen shrinkage was measured at 50 K intervals to 2023 K. After keeping the specimen at this temperature for 15 min, its shrinkage was measured again.

Next, the specimen was cooled to room temperature and put into a carbonate resin holder. One end surface was polished using polishing papers from #400 to #1100. Then, this polished end surface was ion-etched with 4000 V for about 15 min. The microstructure of the etched surface was observed with an optical microscope.

3. Results

The lengths of four specimens during the heating are shown as functions of temperature and time in Fig. 3. It can be seen that the decrease, namely the shrinkage, begins from nearly 1273 K in specimens 3 and 4 containing high residual carbon content,

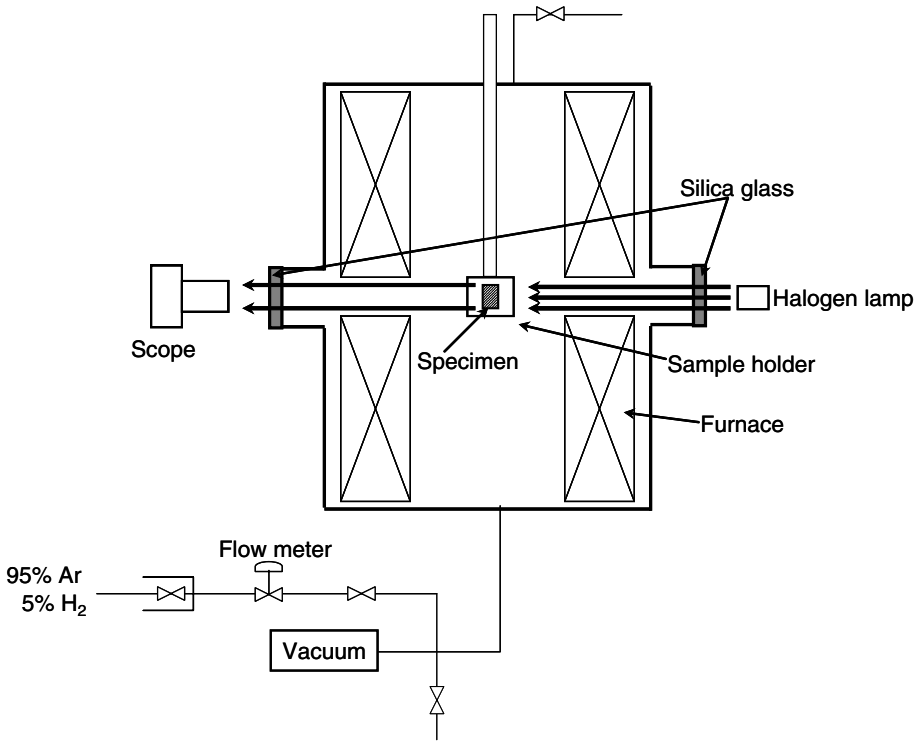

Fig. 2. A schematic diagram of dilatometric measurement system.

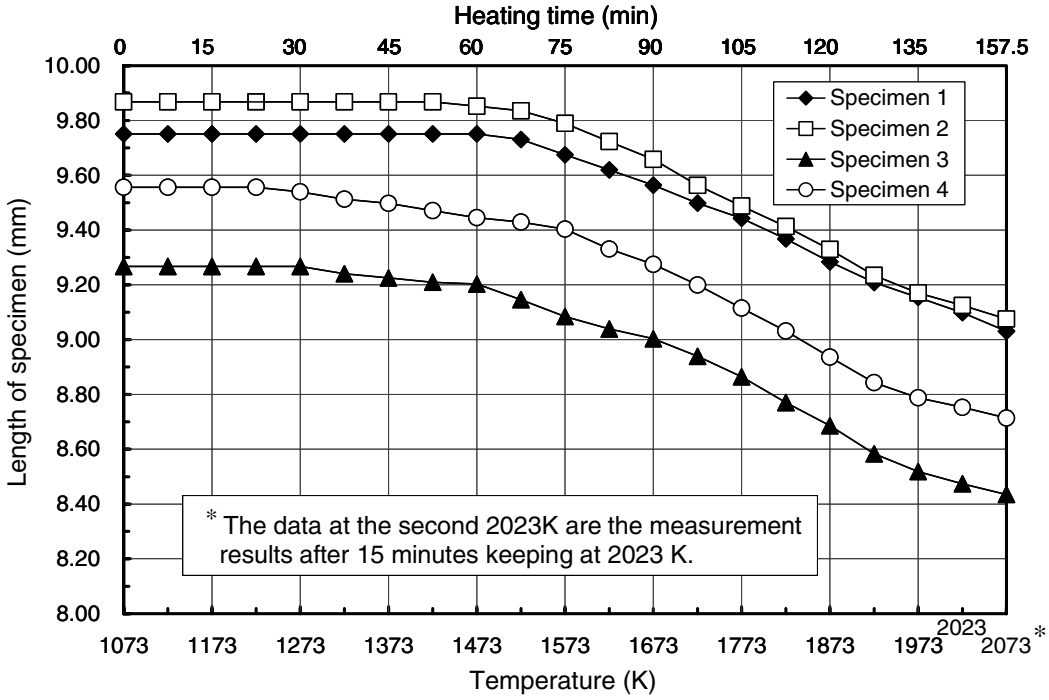

Fig. 3. Length change of specimens during heating.

but it begins at nearly 1473 K in specimens 1 and 2 containing low content. In order to clearly show these differences, the shrinkage rates ($\delta L/L_0$) of four specimens are shown as a function of temperature in Fig. 4, where L_0 is the initial length of specimen before heating and δL is the length change of specimen during each heating interval. On the basis of measured δL and the initial density of specimen, D_0, the densities of specimens during heating are calculated by Eq. (1) and are shown as a function of temperature in Fig. 5. Here it is assumed that the radius and length of the specimen shrink isotropously.

$$D_i = \alpha D_0/(1 - \delta L_i/L_0)^3. \quad (1)$$

D_i: Density of specimen during heating

D_0: Density of specimen before heating

δL_i: Shrunk length of specimen during heating

α: Correction factor

The correction factor α is derived from Eq. (2), and their values are from 1.05 to 1.06.

$$\alpha = D_f/(D_0/(1 - \delta L_f/L_0)^3). \quad (2)$$

Here D_f and δL_f are the density and shrunk length of specimen after heating.

Fig. 6 shows ceramographic images of specimens containing high and low contents of residual carbon. Because the average grain sizes of both specimens measured from these ceramographic observations are about 5 μm, no distinct differences are observed between both grain size and porosity. The final dimensions, geometrical density, carbon content and O/M ratio of each specimen are shown in Table 2 with their initial values.

The following characteristics can be seen by summarizing the above results:

(1) The shrinkage of specimens with high residual carbon content began from 1273 K and this temperature was about 200 K lower than the one at which the specimens with low content began to shrink (Fig. 4).
(2) Densification continued while the specimens were kept at 2025 K; this was especially pronounced for specimens 1 and 2 with low carbon content (Fig. 5).
(3) The carbon content of all specimens after sintering was below the detection limit. The residual carbon in the MOX pellets after de-waxing was completely removed during heating (Table 2).
(4) The O/M ratios in all specimens after sintering were the same value of 1.94 (Table 2).

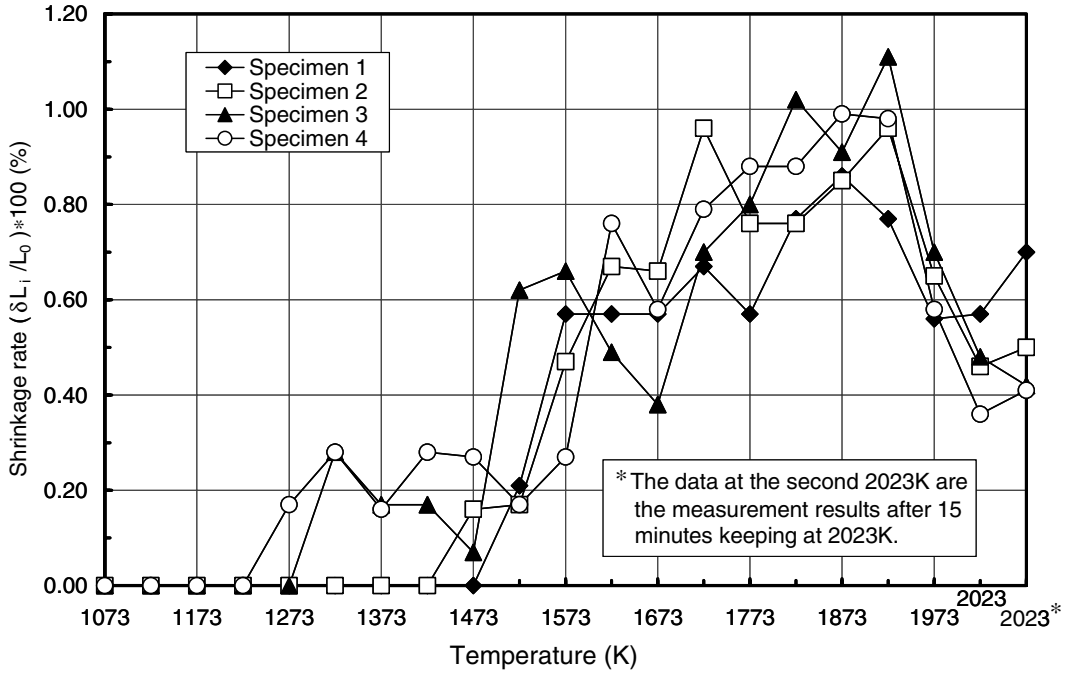

Fig. 4. Shrinkage rates of specimens during heating.

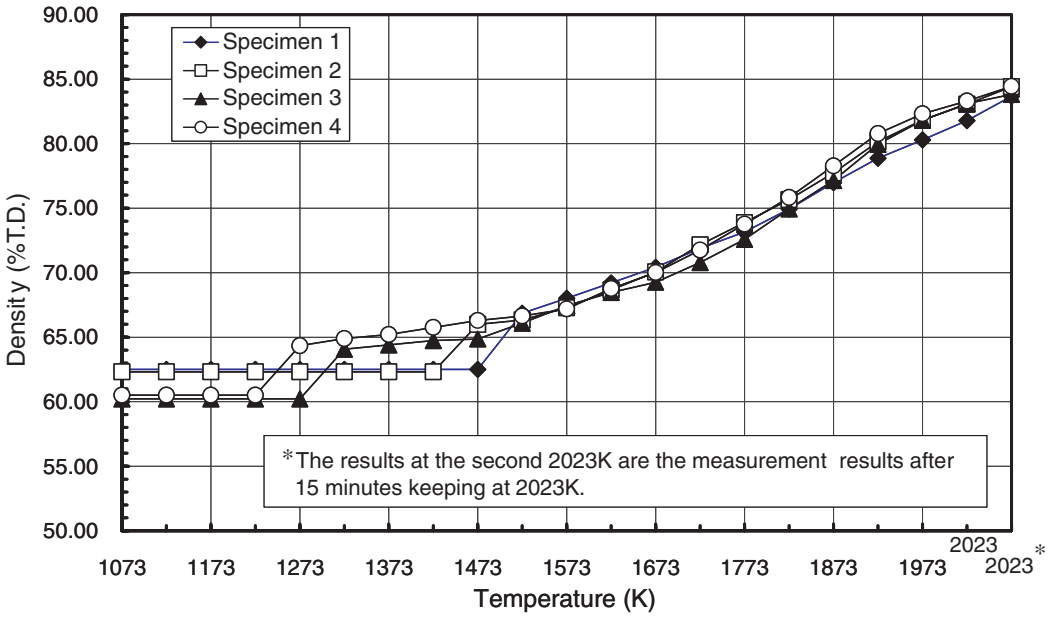

Fig. 5. Calculated densities of specimens during heating.

4. Discussion

4.1. Evaluation of O/M ratio in specimens

It was observed that high carbon content MOX pellets de-waxed in Ar + 5% H_2 gas showed higher radius shrinkage than low content pellets de-waxed in CO_2 gas during sintering in some large scale test fuel fabrication runs of JNC. In order to clarify the reason for this phenomenon, four specimens, two de-waxed in Ar + 5% H_2 gas and two de-waxed in CO_2 gas, were heated to 2023 K from room

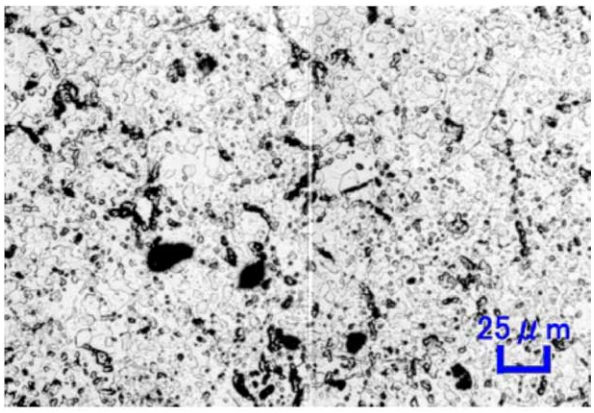

Specimen 1 (carbon content : 290 ppm)

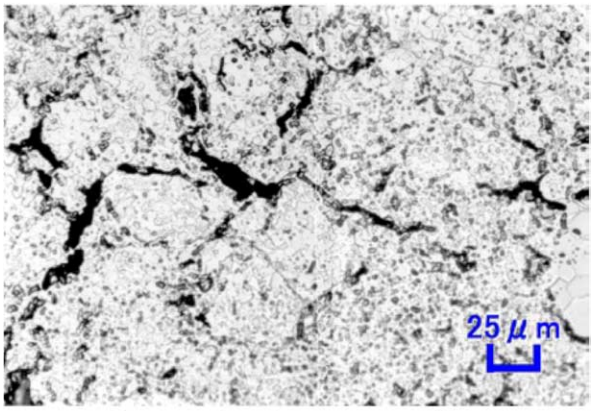

Specimen 3 (carbon content : 1730 ppm)

Fig. 6. Ceramographic images of specimens after heating.

temperature at a heating rate of 400 K/h in Ar + 5% H_2 gas containing 100 ppm of moisture in this study. Their initial O/M ratios were from 2.03 to 2.11 and the specimens with high residual carbon had a higher O/M ratio. During heat treatment, specimens were being reduced to the O/M ratio equilibrated with the oxygen partial pressure given by the atmospheric gas and this O/M ratio significantly affected the diffusion of metal in MOX pellets. Therefore, the O/M ratio of a specimen equilibrated with oxygen partial pressure in Ar + 5% H_2 gas containing 100 ppm of moisture was calculated on the basis of the Blackburn model [10,11]. The oxygen partial pressure was given by the atmospheric gas and was obtained from the standard free energy of formation of H_2O, ΔG^0, shown in Eq. (3) and the equilibrium constant K_p.

$$H_2 + 1/2O_2 \rightarrow H_2O, \quad \Delta G^0 = -58900 + 13.10 * T\,(\mathrm{K}), \tag{3}$$

$$P(H_2O)/(P(H_2) * P(O_2)^{1/2}) = K_p = \exp(-\Delta G^0/RT). \tag{4}$$

Here R is the gas constant and T is temperature.

$$P(O_2) = (P(H_2O)/P(H_2))^2 * (1/K_p)^2. \tag{5}$$

The calculated results of O/M ratios for the four specimens at temperatures from 1073 to 2023 K based on the above equations are shown in Fig. 7 and at 1073 K, 1273 K and 2023 K are 1.998, 1.99 and 1.94, respectively. The calculated O/M ratio of the specimens at 2023 K, 1.94, agrees well with the measured O/M ratio after heating as shown in Table 2.

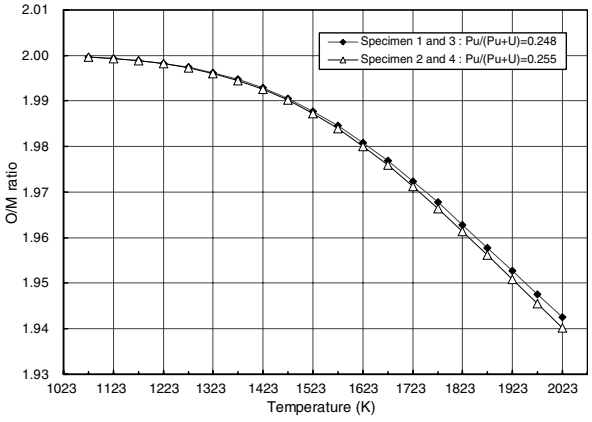

Fig. 7. Calculated O/M ratios of specimens during heating.

Table 2
Characteristics of MOX pellets before after heating

Specimen no.	Diameter (mm)		Length (mm)		Weight (g)		Density (% TD)		Carbon content (ppm)		O/M ratio	
	Before	After	Before	After	Before	After	Before	After	Before	After	Before	After
Specimen 1	6.033	5.406	9.751	9.030	1.920	1.911	62.50	83.67	290	<30[a]	2.03	1.94
Specimen 2	6.092	5.442	9.868	9.076	1.975	1.964	62.31	84.42	560	<30	2.04	1.94
Specimen 3	6.162	5.455	9.267	8.435	1.834	1.821	60.22	83.82	1730	<30	2.09	1.94
Specimen 4	6.163	5.443	9.556	8.714	1.901	1.887	60.51	84.45	1735	<30	2.11	1.94

[a] 30 ppm is the detection limit for carbon content analysis.

As Lambert and Strain [12] reported, the diffusion coefficient of oxygen in the MOX fuel with hyperstoichiometry is as fast as about 10^{-6} cm^2/s at around 1273 K. Thus, the O/M ratio of specimen is expected to reach the value equilibrated with the oxygen partial pressure given by the atmospheric gas in the initial stage of heating and it is reasonable to exclude the effect of initial O/M of specimen on the sintering behavior.

4.2. Formation of carbon monoxide (CO)

Suzuki et al. [13] investigated the fabrication process of mixed carbide of uranium and plutonium given by reaction (6). They found that CO gas began to be released from the powder mixture of UO_2, PuO_2 and graphite at 1270 K and two peaks appeared at 1420 K and 1720 K in the plot showing the temperature dependency of the released amount of CO gas from specimens.

$$(0.8\mathrm{U} + 0.2\mathrm{Pu})\mathrm{O}_2 + 2.98\mathrm{C} \rightarrow (\mathrm{U}_{0.8}\mathrm{Pu}_{0.2})\mathrm{C}_{0.99}\mathrm{O}_{0.01} + 1.99\mathrm{CO}. \quad (6)$$

Here, UO_2, PuO_2 and graphite were mixed at the atomic ratios of Pu/(Pu+U) = 0.20 and C/(Pu+U) = 2.98. The materials and element on the left and right sides of Eq. (6) are the initial reactants and final reaction compounds, respectively. Suzuki et al. [14] have reported in another study on the preparation of plutonium carbide from PuO_2 that the reduction reaction (7) took place as the formation reaction of CO gas at low temperature before formation of carbide at high temperature. If this reduction reaction takes place in the MOX, the shrinkage behavior results obtained in this study can be understood from the viewpoint of O/M dependence of the uranium or plutonium diffusion coefficient in MOX fuel.

$$\mathrm{PuO}_2 + x\mathrm{C} \rightarrow \mathrm{PuO}_{2-x} + x\mathrm{CO}. \quad (7)$$

In this study, the specimen carbon contents were from 290 to 1735 ppm but after heat treatment they were under the detection limit, 30 ppm. It is, therefore, reasonable that the amounts of carbon in the specimens were too low to form plutonium or uranium carbide, because the residual carbon is considered to be completely removed from the specimen as the result of formation of CO gas by Eq. (7). As shown in Fig. 3, the specimens with high residual carbon content began to shrink at about 1273 K, but the specimens with low content began to do so around 1500 K. Furthermore, the data summarized in Table 3 show that shrinkage rate is higher in the specimens with high residual carbon content than in the ones with low residual content in the temperature range from 1273 to 1523 K. This temperature range includes the first peak of CO gas evolution reported by Suzuki et al., although there is no significant difference in shrinkage rate between specimens with high and low carbon contents above 1523 K (Table 3).

Table 3
Shrinkage of specimens

Specimen no.	Shrinkage (%)	
	1273–1523 K	1523–2023 K
Specimen 1	0.21	6.48
Specimen 2	0.33	7.20
Specimen 3	1.31	7.25
Specimen 4	1.33	7.07

Therefore, the shrinkage behavior results obtained in this study can be understood from the viewpoint of O/M dependence of the uranium or plutonium diffusion coefficient in MOX fuel.

4.3. Decrease of O/M ratio by formation of CO gas and consequent increase of metal ion inter-diffusion coefficient

Baptiste and Gallet [15] have investigated the O/M dependence of metal ion inter-diffusion coefficient (described as the inter-diffusion coefficient hereafter) in MOX fuel and showed that the inter-diffusion coefficient was the smallest near O/M = 1.99, but sharply increased with the deviation of O/M ratio from this value at 1873 and 2178 K. Assuming that this relationship between the O/M ratio and inter-diffusion coefficient holds at other temperatures, it is easy to understand why the specimen with higher residual carbon content showed a larger shrinkage rate from 1273 to 1523 K as follows.

In this study, the calculated O/M ratio of specimens based on the Blackburn model is 1.99 at 1523 K (Fig. 7). As mentioned above, the inter-diffusion coefficient has the smallest value at O/M = 1.99. Nevertheless, in Fig. 4, specimens 3 and 4 with high residual carbon content showed the first shrinkage peak at about 1400 K. This behavior can be understood by considering that shrinkage of specimens with high residual carbon content is enhanced from 1273 K to 1523 K by the decrease of O/M ratio due to the evolution of CO gas and

consequently the significant increase of the inter-diffusion coefficient. In the specimens with low residual carbon content, the amount of CO gas evolution was too small to affect the inter-diffusion coefficient.

When the shrinkage begins in the compact specimen while the temperature is being increased, the particle or grain size increases with time. It is, therefore, very hard to evaluate the effect of CO gas evolution and consequently the decrease of O/M ratio on the inter-diffusion in a time interval until oxygen potential in the specimen reaches equilibrium with the oxygen potential of the flowing gas.

Therefore, the shrinkage of specimens can be theoretically evaluated based on the model for the initial sintering stage as one approach to qualitative analysis. It is well known that shrinkage of a compact is proportional to the two-fifths power of the diffusion coefficient in ceramic systems as shown in Eq. (8) [16].

$$\delta V/V_0 = \beta\delta L/L_0 = \beta(20\gamma a^3 D^*/2^{1/2}kT)^{2/5} r^{-6/5} t^{2/5}. \quad (8)$$

V_0	initial volume of dewaxed green pellet
δV	shrunk volume of sintered pellet
L_0	initial length of dewaxed green pellet
δL	shrunk length of sintered pellet
β	coefficient (in case of isotropic shrinkage, $\beta = 3$)
γ	surface energy
a^3	atomic volume of diffusing vacancy
D^*	self-diffusion coefficient
k	Boltzmann constant
T	temperature
r	grain size
t	sintering time

The value of β in Eq. (8) is 3 for isotropic shrinkage. In the ceramic system where the diameter shrinkage is greater than the length shrinkage, β is more than 3. And β is less than 3 for the opposite condition. Table 4 shows the measured shrinkages of diameter, length and volume in four specimens after the final heat treatment, together with the ratio of volume to length shrinkages. These ratios do not differ much from each other. It is, therefore, reasonable to evaluate the shrinkage of specimens by Eq. (8) in this study. Because four specimens were prepared and heated by the same procedures, only the diffusion coefficients are different in Eq. (8). Although the decrease of O/M ratio can not be exactly evaluated during heating, the diffusion coefficient increases by one to three orders of magnitude with the decrease of O/M ratio according to Baptiste and Gallet [15]. It is, then, assumed that the inter-diffusion coefficient in the specimens with high residual carbon content is two orders of magnitude larger than the one with the low residual carbon content. Here, the ratio of shrinkage between specimens evaluated by Eq. (8) is as follows:

$$(\delta V'/V_0')/(\delta V/V_0) = (\beta\delta L'/L_0')/(\beta\delta L/L_0), = (1E(2))^{2/5} = (100)^{2/5} = 6.3. \quad (9)$$

V' and L' are volume and length of a specimen with high residual carbon content and the V and L are the same terms of a specimen with low content. The obtained ratio means that the specimens with high residual carbon content shrink about six times more than the specimens with low content at temperature from 1273 to 1523 K and this value agrees well with the experimental results shown in Table 3.

Table 4
Shrinkage and ratio of volume to length shrinkages

Specimen no.	Shrinkage (%)			Volume shrinkage/Length shrinkage
	Diameter	Length	Volume	
Specimen 1	10.39	7.39	25.64	3.47
Specimen 2	10.67	8.03	26.61	3.31
Specimen 3	11.47	8.98	28.67	3.19
Specimen 4	11.68	8.81	28.87	3.28

5. Conclusion

The effect of carbon remaining in MOX pellets after dewaxing on the sintering behavior was investigated. Specimens containing four different residual carbon contents were prepared and then sintered at 400 K/h from 1073 to 2023 K in an atmosphere of Ar + 5% H_2 mixture gas containing 100 ppm of moisture. The dimensional change of specimens during sintering was measured by a non-contact optical dilatometer.

The specimens with large residual carbon content (over 1730 ppm) began to shrink at nearly 1200 K, but those with small residual carbon content (below 560 ppm) began to do so at about 1450 K. In addition, the shrinkage in the temperature region from 1273 to 1523 K was about six times larger in the former specimens than in the latter specimens.

These results could be understood from the difference of CO gas formation between both type

specimens. That is, in the specimens with large residual carbon content, the large amount of CO gas formation reduced the O/M ratio and consequently increased the inter-diffusion coefficient resulting in the enhanced shrinkage. On the other hand, the CO formation was small in the specimens with small residual carbon content and its effect on the O/M ratio was not so large.

Acknowledgements

The authors wish to express their thanks to Dr Furuya, Professor Emeritus of Kyushu University, for valuable discussions and comments. The authors are also grateful to Dr Nagai for valuable suggestions.

References

[1] W.K. Biermann, H.J. Heuvell, S. Pilate, Y. Vanderborck, E. Pelckmans, G. Vanhellemont, H. Roepenack, W. Stoll, Nucl. Technol. 78 (1987) 278.
[2] J. Krellmann, Nucl. Technol. 102 (1993) 18.
[3] D. Haas, A. Vandergheynst, J.V. Vliet, R. Lorenzelli, J.L. Nigon, Nucl. Technol. 106 (1994) 60.
[4] H.M. MacLeod, G. Yates, Nucl. Technol. 102 (1993) 3.
[5] H. Bariot, J.V. Vallet, G. Chiarelli, J. Edwards, S. Nagai, F. Reshetnikov, IAEA-SM 358 (VII) (1999) 81.
[6] K. Dengschrz, J. Krellmann, J.M. Leblanc, H. Roepenack, G. Venhellemont, ENC 4 FORATOM IX 4 (1986) 41.
[7] K. Hirai, T. Hosokawa, R. Yuda, K. Ueno, Y. Shirai, H. Harada, T. Kogai, T. Kubo, J.H. Davies, in: in: Proc. the Int. Topical Meeting on LWR Fuel Performance, ANS, 1997, p. 490.
[8] B. Julien, C. Delafoy, V. Rebeyrolle, S. Beguin, S. Lansiart, in: Proc. the 2004 Int. Meeting on LWR Fuel Performance (2004) 323.
[9] T. Okita, N. Aono, K. Asakura, Y. Aoki, T. Ohtani, IAEA-SM 358/3 (1999) 109.
[10] P.E. Blackburn, J. Nucl. Mater. 46 (1973) 244.
[11] P.E. Blackburn, C.E. Johnson, IAEA-SM 190/50 (1975) 17.
[12] J.D.B. Lambert, R. Strain, Oxide Fuels, in: R.W. Cahn, P. Hassen, E.J. Kramer (Eds.), Material Science and Technology, 10A, VCH, Germany, 1994, Chapter 3.
[13] Y. Suzuki, Y. Arai, T. Sawayama, J. Nucl. Sci. Technol. 20 (1983) 603.
[14] Y. Suzuki, Y. Arai, T. Sawayama, H. Watanabe, J. Nucl. Mater. 101 (1981) 200.
[15] P.J. Baptiste, G. Gallet, J. Nucl. Mater. 135 (1985) 105.
[16] W.D. Kingery, H.K. Bowen, D.R. Uhlmann, Introduction to Ceramics, second ed., John Wiley & Sons, New York, 1976.